Structural characterization of the Co/Cr multilayers by x-ray-absorption spectroscopy

Y. H. Liou,[1] W. F. Pong,[1,*] M.-H. Tsai,[2] K. H. Chang,[1] H. H. Hseih,[1] Y. K. Chang,[1] F. Z. Chien,[1] P. K. Tseng,[1] J. F. Lee,[3] Y. Liou,[4] and J. C. A. Huang[5]

[1]*Department of Physics, Tamkang University, Tamsui 251, Taiwan*

[2]*Department of Physics, National Sun Yat-Sen University, Kaohsiung 804, Taiwan*

[3]*Synchrotron Radiation Research Center, Hsinchu Science-based Industrial Park, Hsinchu 300, Taiwan*

[4]*Institute of Physics, Academic Sinica, Taipei 115, Taiwan*

[5]*Department of Physics, National Cheng Kung University, Tainan 701, Taiwan*

(Received 11 November 1999; revised manuscript received 4 May 2000)

We have performed Cr and Co *K*-edge x-ray-absorption measurements to investigate the dependence of local electronic and atomic structures on the Cr-layer thickness in epitaxial Co($1\bar{1}00$) (40 Å)/Cr(211) (t_{Cr}) (t_{Cr} = 2, 3, 5, 7, and 9 Å) multilayers. The Cr *K* x-ray-absorption near-edge fine structure (XANES) spectra of the Co/Cr multilayers indicate an abrupt transition of the Cr layer from hcp to bcc structure when the thickness of the Cr layer is increased to exceed ~5 Å or three atomic layers. Our results offer an upper limit for the ability of the Co/Cr interface to stabilize the hcp structure in the thin Cr layer. The numbers of nearest-neighbor and next-nearest-neighbor atoms in the Cr and Co layers determined by extended x-ray-absorption fine-structure measurements performed at the Cr and Co *K* edge, respectively, are consistent with the XANES results.

Magnetic multilayers have attracted a great deal of attention over the last decade because of their peculiar magnetic properties and their technological and fundamental importance.[1] The oscillatory variation of the interlayer exchange coupling with respect to the separation between two ferromagnetic layers in the multilayer systems is particularly of interest.[2] For epitaxial Co/Cr multilayers, previous works showed that the magnetic properties have the characteristics of giant and anisotropic magnetoresistance.[3–5] It was also found that the magnetic and magnetotransport properties of the magnetic multilayers are strongly affected by their electronic and atomic structures.[6] The reflection high-energy electron diffraction (RHEED) analyses by Vavra *et al.*[7] and Henry *et al.*[8] showed that the Cr layer in epitaxial Co/Cr multilayers exhibited an abrupt transition from bcc structure to close-packed structure (fcc or hcp) at a Cr-layer thickness of $\leqslant$ 5 Å. This property was attributed to the interfacial energy that stabilizes the thermodynamically less favored densest atomic arrangement. However, they obtained different local atomic structures around Cr when the Cr layer is very thin. Vavra *et al.* found that pseudomorphically grown Cr layers are constrained coherently to the hcp structure of the underlying Co, while Henry *et al.* reported that no pseudomorphism occurs at the Cr/Co interface, but it is more likely that interdiffusion resulted in forming a close-packed CoCr alloy. Another investigation also found the existence of interdiffusion at the Cr/Co interface of the sputtering grown Co/Cr multilayers.[9,10] Different orientations and preparation conditions of the thin-film samples used in these studies might be the cause of the different interfacial structures. The mismatch of the atomic arrangement at the interface depends on the orientation of the multilayers. Recently, based on structural characterization Huang *et al.*[3] found that though bcc and hcp structures have different atomic arrangements, Co($1\bar{1}00$) and Cr(211) planes match extremely well in symmetry and lattice parameters. In this crystal orientation, the existence of fcc Co/Cr-alloy structure at the interface may not be likely because the fcc structure is incompatible with either hcp($1\bar{1}00$) or bcc(211) atomic arrangement. The x-ray-absorption spectrum is very sensitive to the local environment around the absorbing atom, which can be used as a fingerprint of the crystallographic structure and allows us to study the local structures in multilayer systems.[11,12] In this work we measure the local electronic and atomic structures of a series of Co/Cr multilayers and characterize the variation of local electronic and atomic structures with respect to the Cr-layer thickness. This study may help us understand the dependence of the local electronic and atomic structures in the epitaxial Co/Cr multilayers on the Cr-layer thickness.

X-ray absorption spectra of the Co/Cr multilayers were measured using a double-crystal Si(111) monochromator at the wiggler beamline, with an electron-beam energy of 1.5 GeV and a maximum stored current of 200 mA at the Synchrotron Radiation Research Center (SRRC) in Hsinchu, Taiwan. The absorption spectra of the Co/Cr multilayers and thin-film CoCr alloy at the Cr and Co *K* edges were measured using the fluorescence mode with the Lytle detector at room temperature. The spectra of the reference Cr and Co foils were obtained in transmission mode. All the spectra were collected with step energy of 0.5 eV in the x-ray-absorption near-edge structure (XANES) region and of 2 eV in the extended x-ray-absorption fine-structure (EXAFS) region. Samples of $24x$[Co (40 Å)/Cr (2 Å)] and $20x$[Co (40 Å)/Cr (t_{Cr})] multilayers with t_{Cr} = 3, 5, 7, and 9 Å and a ~50 Å Mo buffer were deposited on the MgO(110) substrates. X-ray-diffraction results indicate that the Co and Cr layers deposited in the alternating Co/Cr multilayers mainly have hcp/bcc structure in the Co($1\bar{1}00$)/Cr(211) orientation. The details of the preparation of the Co/Cr multilayers and x-ray-diffraction determination of the orientation of these multilayers have been described elsewhere.[3–5]

Figures 1 and 2 show, respectively, the Cr and Co *K*-edge XANES spectra obtained for the Co/Cr multilayers, refer-

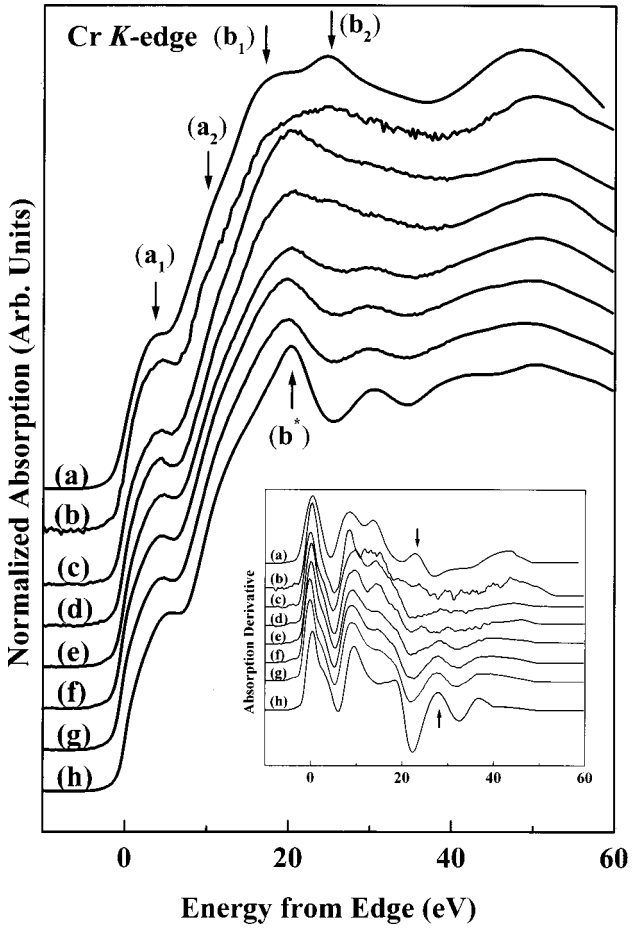

FIG. 1. Normalized Cr K near-edge absorption spectra for epitaxial Co (40 Å)/Cr (t_{Cr}) (t_{Cr}=2, 3, 5, 7, and 9 Å) multilayers. (a) Co foil (offset Co K edge), (b) CoCr alloy, (c) t_{Cr}=2 Å, (d) t_{Cr}=3 Å, (e) t_{Cr}=5 Å, (f) t_{Cr}=7 Å, (g) t_{Cr}=9 Å, and (h) Cr foil.

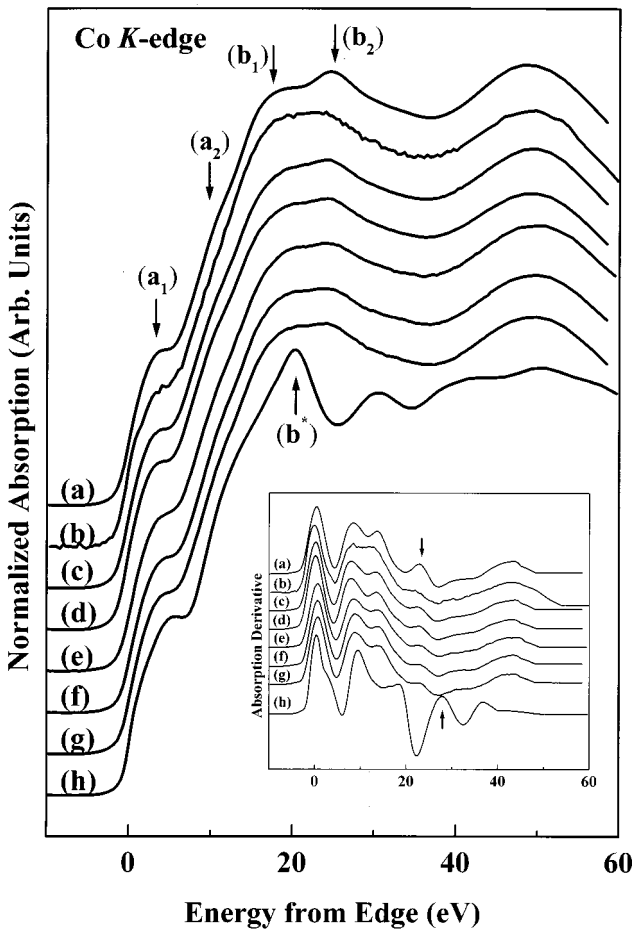

FIG. 2. Normalized Co K near-edge absorption spectra for epitaxial Co (40 Å)/Cr (t_{Cr}) (t_{Cr}=2, 3, 5, 7, and 9 Å) multilayers. (a) Co foil, (b) CoCr alloy, (c) t_{Cr}=2 Å, (d) t_{Cr}=3 Å, (e) t_{Cr}=5 Å, (f) t_{Cr}=7 Å, (g) t_{Cr}=9 Å, and (h) Cr foil (offset Cr K edge).

ence CoCr alloy, and Cr and Co foils. For all the spectra, zero energy was selected at the inflection point of the threshold in the spectra. The zero energies correspond to absolute energies of 5989.0 and 7709.1 eV, respectively, for the Cr and Co K edges. Due to the bulk sensitivity of fluorescence measurements, the spectra in Figs. 1 and 2 predominantly reflect the bulk absorption of the Co/Cr multilayers. The normalized EXAFS oscillations $\chi(k)$ are weighted by k^3 for both Cr and Co K edges, and the corresponding Fourier transforms (FTs) of the $k^3\chi$ data for the Co/Cr multilayers and reference samples are shown in Figs. 3 and 4, respectively. Further analysis involved the use of a combination of the multiple-scattering EXAFS computer program FEFF6 (Ref. 13) and the nonlinear least-squares-fitting computer program FEFFIT.[14] As also shown in Figs. 3 and 4, the quality of the fit for the nearest-neighbor (NN) and next-nearest-neighbor (NNN) bond lengths is quite good.

The part of the Cr K-edge XANES spectra of the Co/Cr multilayers, reference CoCr alloy, and Cr foil and of the offset Co K-edge XANES spectra of the Co foil between labels b_1 and b_2 as shown in Fig. 1 can be attributed to the dipole $1s$-to-$4p$ transitions above the Fermi level. The two small bumps in the region from about 0 to 10 eV above the edge (labeled as a_1 and a_2) are primarily due to the Cr and Co $1s$-to-$3d$ transition through the Cr and Co p-d rehybridization.[15] The two-peak features b_1 and b_2 (labeled by vertical arrows) in the Cr K-edge XANES of the Co/Cr multilayers with a Cr-layer thickness t_{Cr} less than 5 Å closely resemble those of the Co foil with a hcp structure. In contrast, the single-peak feature in the Cr K-edge spectra of the Co/Cr multilayers with $t_{Cr}>5$ Å resembles the single sharp feature b^* located in the region between peaks b_1 and b_2 in the spectrum of the Cr foil with a bcc structure. The features in the Cr K-edge XANES of the CoCr alloy are much broader and appear to be least resolved in comparison with those of the Co/Cr multilayers and Cr and Co foils. The first derivatives of the XANES spectra of the Co/Cr multilayers, CoCr alloy, and Cr and Co foils are shown in the inset of Fig. 1. A general trend of the change from the single peak b^* to the double peaks b_1 and b_2 can be easily seen when the Cr-layer thickness decreases in the Co/Cr multilayers. This trend clearly indicates a local structural transition at $t_{Cr}\sim 5$ Å in the Co/Cr multilayers. It may suggest that pseudomorphic Cr films can be grown on Co and can be constrained coherently into the hcp structure in thin layers ($t_{Cr}<5$ Å). In contrast, the Cr layer prefers to be bulk like when its thickness is greater than 5 Å. The intensity of bumps a_1 and a_2 in the Cr K-edge XANES spectra remains nearly constant. The Co K-edge XANES spectra of the Co/Cr multilayers shown in Fig. 2 contain relatively well-

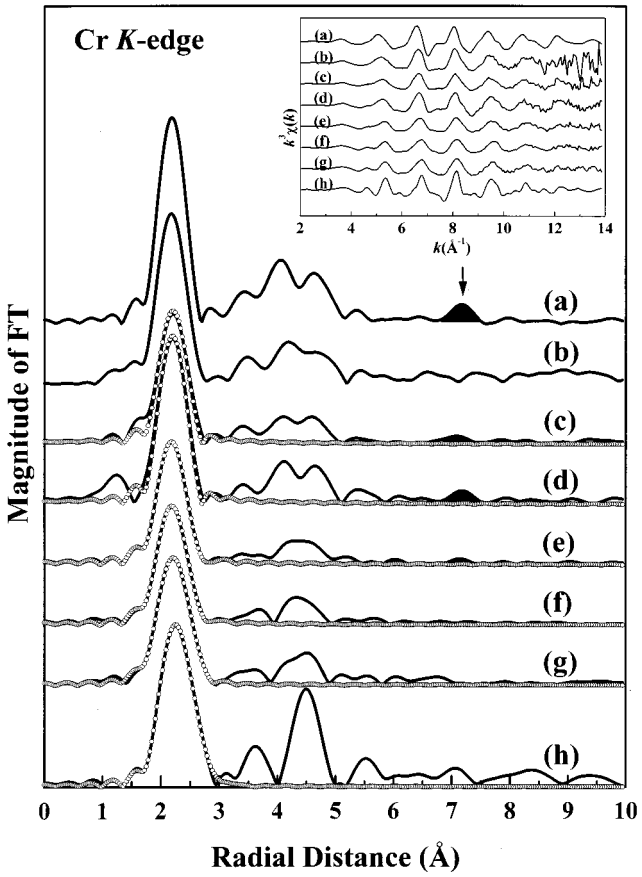

FIG. 3. Fourier transform amplitudes of the EXAFS $k^3\chi$ data at the Cr *K* edge for Co/Cr multilayers. (a) Co foil, (b) CoCr alloy, (c) $t_{Cr}=2$ Å, (d) $t_{Cr}=3$ Å, (e) $t_{Cr}=5$ Å, (f) $t_{Cr}=7$ Å, (g) $t_{Cr}=9$ Å, and (h) Cr foil. Final fit of theory to the NN and NNN bond lengths (open circles). The inset represents the Cr *K*-edge EXAFS oscillation $k^3\chi$ data. In fitting a model compound to the experimental EXAFS, the coordination number of NN Co was fixed at 12 for $t_{Cr}<5$ Å with a hcp structure, while the coordination numbers of NN Cr and NNN Cr were fixed at 8 and 6, respectively, for $t_{Cr}>5$ Å with a bcc structure.

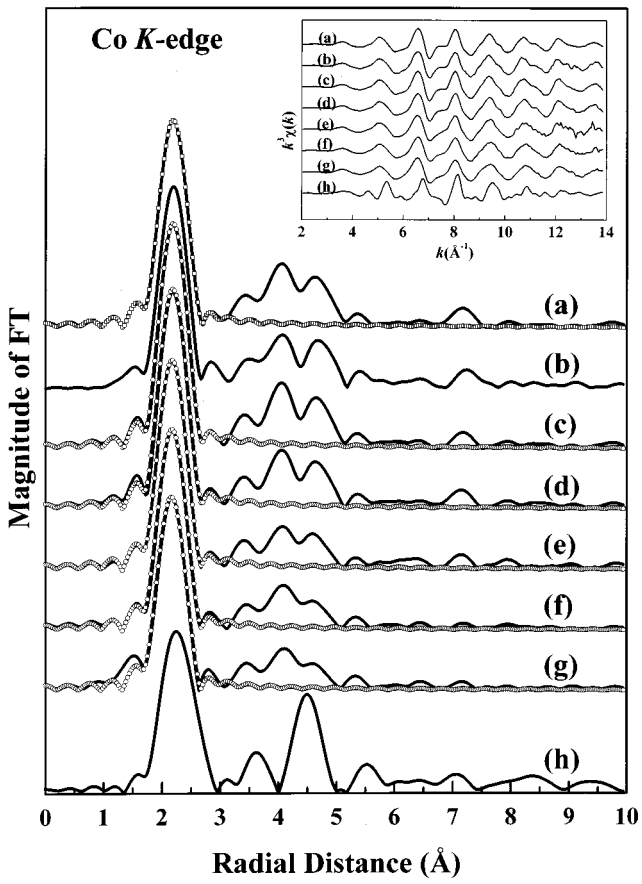

FIG. 4. Fourier transform amplitudes of the EXAFS $k^3\chi$ data at the Co *K* edge for Co/Cr multilayers. (a) Co foil, (b) CoCr alloy, (c) $t_{Cr}=2$ Å, (d) $t_{Cr}=3$ Å, (e) $t_{Cr}=5$ Å, (f) $t_{Cr}=7$ Å, (g) $t_{Cr}=9$ Å, and (h) Cr foil. Final fit of theory to the NN bond lengths (open circles). The inset represents the Co *K*-edge EXAFS oscillation $k^3\chi$ data. The coordination number of Co was fixed at 12 in fitting a model compound to the experimental EXAFS because of a very small contribution from Cr atoms.

resolved two-peak features b_1 and b_2, which resemble those of the Co foil. The first derivatives of the Co *K*-edge XANES spectra of the Co/Cr multilayers, CoCr alloy, and Co and Cr foils are also shown in the inset of Fig. 2.

Figures 3 and 4 show the Cr and Co *K*-edge FTs of the $k^3\chi$ data for the Co/Cr multilayers, CoCr alloy, and Cr and Co foils. The first peaks in the FT spectra shown in Fig. 3 appear to have roughly the same location, though they have different heights and full widths at the half maximum. However, the peaks at a distance larger than ~3 Å appear to differ significantly and can be attributed to differences in the average environment in farther away shells between the two $t_{Cr}>5$ Å and $t_{Cr}\leqslant 5$ Å cases. The features in the FT spectra of the Co/Cr multilayers with a thick Cr layer ($t_{Cr}>5$ Å) have a single peak near 4.5 Å. They resemble closely that of the Cr foil with a bcc structure.[11] On the other hand, the local atomic structures of thin Cr layers ($t_{Cr}\leqslant 5$ Å) in the Co/Cr multilayers and CoCr alloy are quite similar to that of the Co foil with a hcp structure. In the region between 6.8 and 7.3 Å in the FT spectra shown in Figs. 3(a) and 3(c)–3(e), the spectra have a common feature marked by shaded peaks. Other spectra do not have this feature. Since the spectra of Figs. 3(a) and 3(c)–3(e) belong to the Co foil and Co/Cr multilayers with thin Cr layers ($t_{Cr}\leqslant 5$ Å), respectively, our FT spectra show that the thin Cr layers ($t_{Cr}\leqslant 5$ Å) are more likely to have the same hcp structure of the Co foil. This agrees with XANES results and further confirms that the epitaxially grown $t_{Cr}\sim 5$ Å Cr layers in the Co/Cr multilayers are constrained to be Co metal like as reported by earlier RHEED studies.[7,8] The similarity between the XANES spectra of the reference CoCr alloy and Co metal suggests that the CoCr alloy has a hcp structure, in agreement with our x-ray-diffraction measurement. The FT spectra shown in Fig. 3 have the characteristic of splitting two-neighbor shells in the region between 3.8 and 5.0 Å for $t_{Cr}\leqslant 5$ Å. The splitting two-neighbor shells are also found in the FT spectra of the Co *K* edge for the Co/Cr multilayers, CoCr alloy, and Co foil as shown in Fig. 4. In Fig. 4 the splitting two-neighbor shells are nearly at the same position for the Co/Cr multilayers, CoCr alloy, and Co foil, but the heights are obviously larger for thinner Cr layers than for thicker Cr layers in the Co/Cr multilayers. This property can be primarily attributed to the decrease of the structural order due to NNN bond-length dis-

tortion in the Co layer caused by the thick bcc Cr layer.

A best-fit procedure is applied to the first main peaks in the Cr *K*-edge EXAFS FT spectra to obtain NN and NNN bond lengths using the one- and two-shell models for $t_{Cr}<5$ Å and $t_{Cr}>5$ Å, respectively. The Cr atoms are found bonded with 12 NN Co atoms at 2.50 ± 0.01 Å, which is a characteristic of the hcp structure, for $t_{Cr}<5$ Å. For $t_{Cr}>5$ Å, the Cr atoms are bonded with 8 NN Cr atoms at 2.49 ± 0.01 Å and 6 NNN Cr atoms at 2.78 ± 0.02 Å for $t_{Cr}=7$ Å and at 2.84 ± 0.02 Å for $t_{Cr}=9$ Å indicative of a bcc structure. The 2.84 Å NNN bond length is close to that of the bulk Cr metal of 2.88 Å. For $t_{Cr}=5$ Å the Cr layer contains ~3 atomic layers of Cr. The central Cr layer is sandwiched between two Cr side layers, so that the nearest neighbors of the atoms in this layer are all Cr atoms. On the other hand, the side-layer Cr atoms have some bcc-type Cr nearest neighbors and some hcp-type Co nearest neighbors. The real sample may even contain both hcp and bcc phases. Thus, in this case, the EXAFS data were fitted with a combination of 1/3 hcp and 2/3 bcc coordinations. The NN and NNN bond lengths obtained are 2.50 ± 0.01 and 2.84 ± 0.02 Å, respectively. They are consistent with those determined for other Cr-layer thicknesses. The single-shell model is fitted for the first main peak of the Co *K*-edge FT spectra for all Co/Cr multilayers. The Co atoms are found bonded with 12 NN Co atoms at 2.49–2.50 Å indicative of a hcp structure.

Transition metals with a fcc structure have a closed or nearly closed outermost *d* shell, while those with a hcp structure have a few singly occupied *d* orbitals.[16] Both fcc and hcp structures are the densest structure, in which each atom has 12 NN atoms and the coupling between atoms are dominated by metallic bonding through itinerant electrons, which are not directional. In contrast, the transition metals with a bcc structure have from 3 to 6 *d* electrons in the outermost *d* shell. Since the 5 *d* orbitals are directional, the contribution of *d* orbitals to the coupling between two neighboring atoms is also directional, which renders the bcc structure with a smaller coordination number of 6 becomes more favorable than the fcc/hcp structure. When the Cr layers are one and two atoms thick and have the hcp $(1\bar{1}00)$ structure of the Co layer, the Cr atoms are coordinated, respectively, with 10 and 8 or 6 Co atoms, which couple with the Cr atoms through itinerant electrons and stabilize the hcp structure. For a three-atom-thick Cr layer, the Cr atoms are coordinated with more Cr atoms than Co atoms; the additional directional Cr-Cr couplings through *d* orbitals render the bcc structure to become more favorable. Based on the above argument, the observed ultrathin (three-atomic-layer) critical thickness of the bcc Cr layer seems to suggest that the interdiffusion of Co and Cr atoms at the interface is less likely or at least is limited to very few layers. The physical reason is that interdiffusion reduces the number of Cr atoms surrounding a given Cr atom and tends to destabilize the bcc structure, so that a thicker Cr layer is required to be stabilized in the bcc structure. Based on structural characterization, Huang *et al.*[3] found that though bcc and hcp structures have different atomic arrangements, Co$(1\bar{1}00)$ and Cr(211) planes match extremely well in symmetry and lattice parameters. The unit cell of Co$(1\bar{1}00)$, $4.07\text{ Å}\times2.51\text{ Å}$, matches perfectly that of Cr(211), $4.07\text{ Å}\times2.50\text{ Å}$. The one-atom-thick hcp Cr$(1\bar{1}00)$ layer is expected to have a similar excellent match and have negligible strain energy. For the two-atom-thick hcp Cr$(1\bar{1}00)$ layer, the strain energy is associated with the distortion of the NN bond angles from those of the bcc Cr(211) structure. For semiconductors the NN bonding is covalent and directional and the bond-angle distortion gives rise to significant strain energy.[17] In contrast, for transition metals the strain energy associated with the bond-angle distortion is given rise by directional *d*-orbital couplings, which is not as significant as the nondirectional metallic bonding through itinerant electrons. Thus the strain energy in the two-atom-thick hcp Cr$(1\bar{1}00)$ layer is of second order. During the deposition of the third Cr layer, this strain energy can be easily overcome by the energy transferred from the adsorption energy of the approaching gas-phase Cr atoms. Thus a three-atom-thick bcc Cr(211) layer can be easily formed.

In summary, our Cr and Co *K*-edge XANES measurements for the epitaxial Co (40 Å)/Cr (t_{Cr}) ($t_{Cr}=2$, 3, 5, 7, and 9 Å) multilayers show an abrupt transition of the Cr layer from hcp structure to bcc structure at ~5 Å. Our results offer an upper limit for the ability of the Co/Cr interface to stabilize the hcp structure in the thin Cr layer. The hcp-to-bcc transition around $t_{Cr}\sim5$ Å is further confirmed by the EXAFS measurements performed at the Cr and Co *K* edge.

One of the authors (W.F.P.) would like to thank the National Science Council of R.O.C. for financially supporting this research under Contract No. NSC 89-2112-M-032-008. SRRC is also appreciated for the use of their wiggler beamline to perform this study.

*Author to whom correspondence should be addressed.

[1] *Ultrathin Magnetic Structures*, edited by J. A. C. Bland and B. Heinrich (Springer-Verlag, Berlin, 1994), Vols. I and II.

[2] S. S. P. Parkin, N. More, and K. P. Roche, Phys. Rev. Lett. **64**, 2304 (1990); M. T. Johnson, R. Coehoorn, J. J. de Vries, N. W. E. McGee, J. aan de Stegge, and P. J. H. Bloemen, *ibid.* **69**, 969 (1992).

[3] J. C. A. Huang, Y. Liou, Y. D. Yao, W. T. Yang, C. P. Chang, S. Y. Liao, and Y. M. Hu, Phys. Rev. B **52**, R13 110 (1995).

[4] J. C. A. Huang, F. C. Tang, W. W. Fang, R. L. Liu, Y. M. Hu, C. K. Lo, Y. Liou, Y. D. Yao, W. T. Yang, C. P. Chang, and S. Y. Liao, J. Appl. Phys. **79**, 4790 (1996).

[5] Y. D. Yao, Y. Liou, J. C. A. Huang, S. Y. Liao, I. Klik, W. T. Yang, C. P. Chang, and C. K. Lo, J. Appl. Phys. **79**, 6533 (1996).

[6] G. A. Prinz, Phys. Rev. Lett. **54**, 1051 (1985); D. P. Pappas, K. P. Kämper, and H. Hopster, *ibid.* **64**, 3179 (1990); E. E. Fullerton, D. M. Kelly, J. Guimpel, I. K. Schuller, and Y. Bruynseraede, *ibid.* **68**, 859 (1992).

[7] W. Vavra, D. Barlett, S. Elagoz, C. Uher, and R. Clarke, Phys. Rev. B **47**, 5500 (1993).

[8] Y. Henry, C. Mény, A. Dinia, and P. Panissod, Phys. Rev. B **47**, 15 037 (1993).

[9] N. Sato, J. Appl. Phys. **61**, 1979 (1987).

[10] P. Boher, F. Giron, Ph. Houdy, P. Beauvillain, C. Chappert, and P. Veillet, J. Appl. Phys. **70**, 5507 (1991).

[11] S. Pizzini, F. Baudelet, D. Chandesris, A. Fontaine, H. Magnan, J. M. George, F. Petroff, A. Barthélemy, A. Fert, R. Loloee, and P.

A. Schroeder, Phys. Rev. B **46**, 1253 (1992); S. Pizzini, F. Baudelet, A. Fontaine, M. Galtier, D. Renard, and C. Marlière, *ibid.* **47**, 8754 (1993).

[12] P. Le Fevre, H. Magnan, O. Heckmann, V. Briois, and D. Chandesris, Phys. Rev. B **52**, 11 462 (1995); P. Le Fevre, H. Magnan, and D. Chandesris, Surf. Sci. **352–354**, 923 (1996).

[13] J. J. Rehr, J. M. deLeon, S. I. Zabinsky, and R. C. Albers, J. Am. Chem. Soc. **113**, 5135 (1991); J. J. Rehr, R. C. Albers, and S. I. Zabinsky, Phys. Rev. Lett. **69**, 3397 (1992).

[14] A. I. Frenkel, E. A. Stern, M. Qian, and M. Newville, Phys. Rev. B **48**, 12 449 (1993).

[15] T. K. Sham, A. Hiraya, and M. Watanabe, Phys. Rev. B **55**, 7585 (1997).

[16] *Table of Periodic Properties of the Elements* (Sargent-Welch Scientific, Skokie, IL, 1990).

[17] W. A. Harrison, *Electronic Structure and the Properties of Solids* (Freeman, San Francisco, 1980).